Journal of Bioenergetics and Biomembranes, Vol. 17, No. 3, 1985

Model for the Electrolytic Environment and Electrostatic Properties of Biomembranes

D. E. Amory[1,2] and J. E. Dufey[1,3]

Received September 10, 1984; revised November 26, 1984

Abstract

Physical and chemical interactions of ions with biomembranes are described by a model originating from the Stern theory. Equations of the model have analytical solutions only for very simple, often unrealistic situations. The numerical resolution adopted permits a much wider application of the model: Potentials and concentrations can be calculated anywhere from the surface and in any electrolytic environment. The model is applied to biomembranes. Simulations are presented in three-dimensional figures which allow one to use the model as a practical research tool. In particular, the simulations reveal that, in practice, it is possible to induce an increase of the surface charge density simultaneously with a decrease of the surface potential, and, theoretically, that the potential at the exclusion distance (which estimates the diffuse layer thickness) exhibits a remarkably constant value as the composition of the free solution is varied.

Key Words: Electrostatic model; membrane binding; numerical surface potential; Stern, Gouy–Chapman models.

Introduction

The electrical properties of solid–liquid interfaces are the key to the fundamental explanation of numerous phenomena relevant to the mineral world as well as to the biological world. That is why researchers working in disciplines so far apart from each other as the physicochemistry of clays and the properties of biological membranes can use the same theoretical models to support the fundamental interpretation of their observations. Among these models, the diffuse double layer theory is the most invoked. In spite of this convergence of theoretical approaches, the references usually cited in the

---

[1] Laboratoire de Physicochimie Biologique, Catholic University of Louvain, Place Croix du Sud 2, 1348 Louvain-la-Neuve, Belgium.

[2] Research Assistant, National Fund for Scientific Research (FNRS Belgium).

[3] Research Associate, National Fund for Scientific Research (FNRS Belgium).

literature produced by these two disciplines are surprisingly scarce and are limited to the first half of this century. They consist almost exclusively of the following papers: Gouy (1910) and Chapman (1913) who established the basis of the model; the works of Stern (1924), Verwey and Overbeek (1948), and Grahame (1947) who improved the initial theory in various aspects so that it is often now named the Stern theory.

It is worthwhile to inquire into the more recent developments of the double layer theory in various fields of research. As the starting point of a cross-bibliography, the works of Van Olphen (1977), Bolt (1979), Arnold (1978), Levine and Outwaithe (1978), McLaughlin (1977), and Carnie and McLaughlin (1983) can be consulted. The Stern theory appears to be especially successful in accounting for the surface phenomena occurring on phospholipid membranes of animal, plant, and (*a fortiori*) materials of synthetic origin. Among these phenomena are:

—the variation of the surface potential as a function of the electrolytic composition of the medium; see, e.g., Ohki and Sauve (1978), Ohki and Kurland (1981), Haynes (1974), Eisenberg *et al.* (1979), McLaughlin *et al.* (1971, 1981), Lau *et al.* (1981), Alvarez *et al.* (1983), McLaughlin *et al.* (1978, 1983), and Ehrenberg and Berezin (1984).

—the membrane ionization as a function of pH; see e.g., Gibrat and Grignon (1982), Lakhdar-Ghazal *et al.* (1983), Caspers *et al.* (1983), and Ferreira *et al.* (1984).

—the control of the activity of various membrane-bound enzymes by the electrolytical medium; see, e.g., Theuvenet and Borst-Pauwels (1976), Roomans and Borst-Pauwels (1978, 1979), Ahrens (1981, 1983), Cunningham and Sinthusek (1979) and Wojtczak and Nalecz (1979).

—the measurement of the surface potential by using a fluorescent probe, 9 aminoacridine (Theuvenet *et al.*, 1984) or anilinonaphthalene sulfonate (Gibrat and Grignon, 1982); a phophorescent probe, the terbium ion (Hashimoto and Rottenberg, 1983); or a cationic spin probe (Hashimoto *et al.*, 1984).

The practical implications of these electrical properties are numerous: They encompass the regulation of some nervous and muscular functions as well as the control of the mineral nutrition of plants.

The purpose of this paper is to present a complete set of data obtained by the application of both the Gouy–Chapman and the Stern model. These simulations describe the properties of a charged surface in contact with an electrolytic solution consisting of the following ions: two cations (monovalent and divalent) accompanied by a unique monovalent anion. Such a composition is very often encountered in studies of biological membranes and presents, as a result, the most general interest.

The advantages of this theoretical approach is stressed by the following points:

—It is useful to examine together all of the properties originating from the formation of a Stern layer and a diffuse layer. In fact, most authors who use the Stern theory only present those aspects of the model which are, strictly, necessary for the interpretation of their experimental data.

—An overview of the different aspects of the model suggests a deeper investigation of the capability of this research tool.

—The figures presented can help the biologist (who is not necessarily a specialist in surface chemistry) to select appropriate experimental conditions for his work. It has in fact been shown that the use of sophisticated mechanisms can sometimes be avoided in order to explain experimental data if electrostatic effects are considered (see, e.g., Theuvenet and Borst-Pauwels, 1976).

—Owing to the three-dimensional presentation (a given property is shown as a function of the monovalent and the divalent cation concentrations), it is possible to see, immediately, the best way to induce the variation of the surface property whose impact on any phenomenon is to be measured: an enzymatic activity (see, e.g., Ahrens, 1981, 1983), the binding of a fluorescent probe (see, e.g., Chiu *et al.*, 1980), the membranes asymmetry (see, e.g., McLaughlin and Harary, 1974), the membrane potential (see, e.g., Robertson and Rottenberg, 1983), etc.

—Much data from the literature have not been submitted to a thorough and quantitative treatment in terms of the Stern theory, more often because of the lack of adequate calculational methods. Nowadays, such problems can easily be resolved with the help of microcomputers. These simulations can, as a result, be the starting point for reevaluating older data.

—The improvement of the Gouy–Chapman theory by considering specific surface-cation bindings poses the question of describing the complexation mechanisms. The simulations permit one to check the adequacy of different choices for the specific binding mechanism of the divalent cation.

Theory

The Boltzmann equation links the concentration of an ionic species M_i in the diffuse layer with the concentration of this species in the free solution:

$$[M^z]_x = [M^z]_\infty \exp(-zF\Psi_x/RT) \qquad (1)$$

In this equation , [ ]'s refer to volume concentrations so called as opposed to surface concentrations (in the Stern layer); Ψ is the electrical potential; x is the space coordinate perpendicular to the charged surface, with $x = \infty$

referring to the free solution; z is the valence of the ionic species; R is the gas constant; and T is the temperature.

The Grahame equation relates the surface charge density σ to the surface potential Ψ_0.

$$\sigma^2 = 2\varepsilon_r\varepsilon_0 RT \sum [\mathrm{M}_i]_\infty(\exp(-z_i F\Psi_0/RT) - 1) \tag{2}$$

In this equation, ε_r is the dielectric constant of the medium, ε_0 is the space permittivity, and the summation concerns all the ionic species in the solution.

There are some major assumptions in the Gouy–Chapman theory and several papers deal about each peculiar point (see, e.g., Carnie and McLaughlin, 1983). In the case of phospholipid membranes, the Stern layer consists of cations fixed by a specific binding to some peculiar site of the membrane (indicated by R). If the sites have a negative charge, the following complexes can occur: $\mathrm{R^-M^+}$ with the monovalent cation; $\mathrm{R^-M^{++}}$ and/or $\mathrm{R^{-2}M^{++}}$ (i.e., $\mathrm{R^-M^{++}R^-}$) with the divalent cation.

The relationship between the surface concentration of these complexes (mol/m^2) and the local concentration of the free ionic species can be described by a Langmuir adsorption equation, which is analogous to the mass action law provided that all the activity coefficients are equal to one (Eisenberg *et al.*, 1979; Lau *et al.*, 1981; Aveyard and Haydon, 1973; Lakhdar-Ghazal *et al.*, 1983).

The eventual variations of the activity coefficients in the following equations as well as in the Boltzmann equation are neglected. This is, among others, a fundamental assumption of the model which does not seem to affect its working value. The activity coefficients of the surface phase must of course be defined if purely thermodynamic considerations are to be applied to adsorption and ion exchange phenomena. Such an approach is uncommon in biological disciplines (Van Cutsem and Gillet, 1981, 1982). On the other hand, thermodynamic is a routine tool in soil science. The latest developments in this field have been presented by Sposito (1981).

For the three kinds of complexes mentioned above, the following equations are thus valid:

$$\{\mathrm{R^-M^+}\} = K_1\{\mathrm{R^-}\}[\mathrm{M^+}]_0 \tag{3}$$

$$\{\mathrm{R^-M^{++}}\} = K_2\{\mathrm{R^-}\}[\mathrm{M^{++}}\}]_0 \tag{4}$$

$$\{\mathrm{R^{-2}M^{++}}\} = K_3\{\mathrm{R^{-2}}\}[\mathrm{M^{++}}]_0 \tag{5}$$

In these equation { }'s refer to surface concentrations and K_1, K_2, and K_3 are intrinsic association constants. The subscript 0 specifies the localization of the volume concentrations which is in the plane $x = 0$ and not in the free solution.

If all R sites bear a unique charge, it can be stated that

$$\{R^{-2}\} = \{R^-\}/2 \tag{6}$$

The R-balance equation can be written as

$$\{R_{tot}\} = \{R^-\} + \{R^-M^+\} + \{R^-M^{++}\} + 2\{R^{-2}M^{++}\} \tag{7}$$

and the surface charge density which must be compensated by the ions of the diffuse layer is given by

$$\sigma = -(\{R^-\} - \{R^-M^{++}\}) \tag{8}$$

By combining Eqs. (3)–(8), the following equation is obtained:

$$\sigma = -\{R_{tot}\}\frac{1 - K_2[M^{++}]_0}{1 + K_1[M^+]_0 + (K_2 + K_3)[M^{++}]_0} \tag{9}$$

Numerical Resolution

The following data have to be introduced in the model: $\{R_{tot}\}$, K_1, K_2, K_3, $[M^+]_\infty$, and $[M^{++}]_\infty$. The quantity $[M^-]_\infty$, the monovalent anion concentration in the free solution, is fixed by application of the electroneutrality requirement.

By successive approximations, the value of Ψ_0 which gives a single value to σ as it is calculated by Eq. (2) or (9) can be determined. In these two equations, the values of $[M^{++}]_0$, $[M^+]_0$, and $[M^-]_0$ are provided by the Boltzmann equation. The surface concentrations $\{R^-\}$, $\{R^-M^+\}$, $\{R^-M^{++}\}$, and $\{R^{-2}M^{++}\}$ can then be calculated readily by combining Eqs. (3)–(8). The values of the electric potential (and consequently of the ionic concentrations) at different distances from the surface are obtained by integration of the equation

$$\left(\frac{\partial\Psi}{\partial x}\right)^2 = \frac{2RT}{\varepsilon_r\varepsilon_0}\sum[M_i]_\infty(\exp(-z_iF\Psi/RT) - 1) \tag{10}$$

In the case of symmetric electrolytes (1–1, 2–2), such an integration is easily performed by means of classic analytical methods. For nonsymmetric electrolytes (2–1), the analytical integration is still possible (Abraham-Schrauner, 1975, 1977) but is rather difficult. A numerical resolution technique is preferred. It offers the advantage of providing a unique solution for a medium consisting of any number and any type of electrolyte. If the space coordinate is divided into equal increments of Δx length, the method of finite difference gives

$$\Psi_j = \Psi_{j-1} \pm \Delta x\frac{2RT}{\varepsilon_r\varepsilon_0}\left(\sum[M_i]_\infty(Y_{j-1} - 1)\right)^{1/2} \tag{11}$$

with

$$Y_{j-1} = \exp(-z_i F \Psi_{j-1}/RT) \tag{12}$$

In these equations, the subscript j refers to the value of any parameter at $x = j\Delta x$ ($j = 1,2, \ldots$). Beginning with the value of Ψ_0, Ψ_1 and $[M^z]_1$ can be calculated. From there, Ψ_2 and $[M^z]_2$ can be calculated, and by successive calculations any Ψ_j and $[M^z]_j$ can be found. In Eq. (11), the positive sign is retained if $\Psi_0 < 0$, and the negative sign if $\Psi_0 > 0$.

The conditions of stability and convergence of this very simple explicit solution (11) have been checked. For this purpose, Ψ values obtained by its application for different values of the increment Δx have been compared to the values obtained by the analytical solution which has been derived for mono-monovalent electrolytic systems (see, e.g., McLaughlin, 1977; Eisenberg *et al.*, 1979). On this basis a distance increment of 0.5 Å has been used throughout all the simulations of this paper. This method results in values of Ψ_x of adequate accuracy (data not shown).

By integrating the concentrations as a function of x, i.e., by calculating the sums

$$\Gamma_i = \sum_{j=1}^{\infty} ([M_i]_j - [M_i]_\infty)\,\Delta x \tag{13}$$

the excess of deficient quantities of each ion i (cations and anions) contributing to the neutralization of the surface charge density are obtained. The composition of the diffuse layer can then be determined. For practical reasons, the procedure is stopped when a value of j providing a value of Ψ_j close to zero is reached. In all simulations, calculations were also stopped when $0.99 < Y_j < 1.01$.

It is worth mentioning that analytical solutions have also been proposed for calculation of Γ_i values (Eriksson, 1952), but similarly to the analytical solutions of Eq. (10) their field of application is inescapably more restricted than numerical solutions. Four combinations of data have been used in the model (Table I). Two different surface charge densities are compared: 0.5×10^{-6} and 2.37×10^{-6} mol/m^2. The latter corresponds to an R-site density of 1/70 (Å^{-2}). It is a value lying in the range commonly encountered with phospholipid membranes. The A and B simulations are the application of the Gouy–Chapman theory (therefore without considering any specific bindings). The C and D simulations are the application of the whole model (Stern theory). They consider three kind of complexes: R^-M^+ and R^-M^{++} in simulations C; R^-M^+ and $R^{-2}M^{++}$ in simulations D. The association constants used were found from the literature; $K_1 = 0.6\,M^{-1}$ corresponds to the specific binding of Na-phosphatidylserine (Eisenberg *et al.*, 1979; Ohki and Kurland, 1981); $K_2 = 8.5\,M^{-1}$ corresponds to Ca-phosphatidylglycerol

Table I. Model Simulations

	Association constants (M^{-1})			
	K_1	K_2	K_3	
Simulations	R^-M^+	R^-M^{++}	$R^{-2}M^{++}$	Surface charge concentration $R_{tot}(10^{-6}\ mol/m^2)$
A	0	0	0	2.37
B	0	0	0	0.5
C	0.6	8.5	0	2.37
D	0.6	0	30	2.37

binding (Lau *et al.*, 1981); $K_3 = 30\,M^{-1}$ is the value established for the Ca-phosphatidylserine complexes (Ohki and Kurland, 1981). Concentrations in the free solution of 0, 10^{-4}, 10^{-3}, 10^{-2}, and 10^{-1} M for the monovalent cation and of 0, 10^{-5}, 10^{-4}, 10^{-3}, 10^{-2}, and 10^{-1} M for the divalent cation were used for all simulations.

Simulations

The Surface Charge Density, σ

The total surface site concentration $\{R_{tot}\}$ is a function of the membrane composition. It can be modified directly by incorporation of ionic surfactants (Haynes, 1974; Wojtczak and Nalecz, 1979) or indirectly by manipulation of the growth environment (Hossack *et al.*, 1972). The surface charge density σ is a function of R_{tot} and of the electrolytic environment if binding mechanisms are involved.

In A and B simulations, it is obvious that the surface charge density remains constant since this is one of the hypothesis of the Gouy–Chapman model. In C and D simulations (Fig. 1), the surface charge density, which is balanced by the ions of the diffuse layer, is always smaller than $\{R_{tot}\}$, since part of the charged sites are neutralized by complexation with M^+ and/or M^{++}.

In the presence of a unique electrolyte ($[M^+]_\infty = 0$ or $[M^{++}]_\infty = 0$), σ remains constant except when the divalent concentration is very high (10^{-1} M). As will be shown later, this is due to the good stability of ionic concentrations at the surface (where $x = 0$) with which the complexed forms are equilibrated [Eqs. (3)–(5)]. The reduction of the surface charge is more important in the presence of divalent cations than in the presence of monovalent cations since the former ions have a greater tendency to form com-

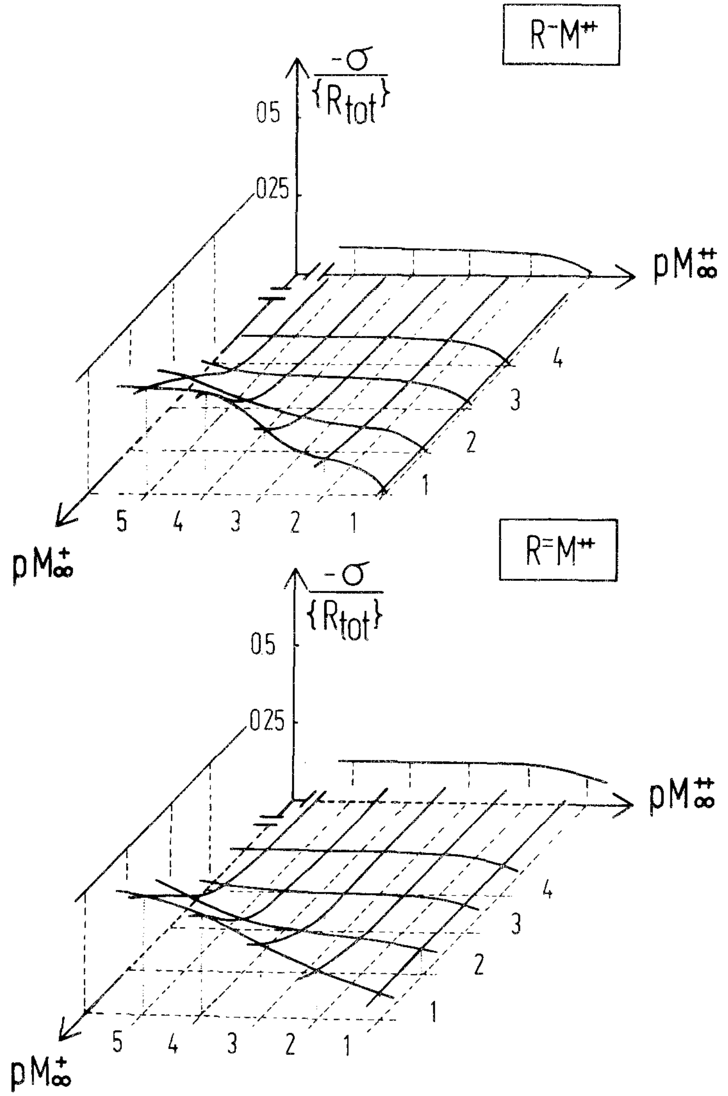

Fig. 1. Ratio of surface charge density to total surface site concentration versus concentration in the free solution of divalent and monovalent cations; $pM^z = -\log[M^z]$ in mol/liter. Two different binding mechanisms are compared (simulations C and D).

plexes with the charged groups of the membrane than the latter ions. When the solution consists of both electrolytes, σ remains constant over a wide range of concentration. Its value is controlled by the presence of the divalent cations and changes under the control of the monovalent cation concentration only in the simultaneous presence of weak $[M^{++}]_\infty$ concentrations and high $[M^+]_\infty$ concentrations.

The complexing mode, R^-M^{++} or $R^{-2}M^{++}$, affects only slightly the shape of the variation. In the range of concentrations where $[M^{++}] < 10^{-2}$ M, it would even be possible to adjust K_2 and K_3 so that identical values of σ are obtained. Nevertheless, there is a fundamental difference between the two binding mechanisms. Due to the positive charge of the R^-M^{++} complex, a sufficient increase of the divalent cation concentration may reverse the sign of the surface charge. This property has been applied successfully to the measure of the association constant K_2 (Lau *et al.*, 1981; McLaughlin *et al.*, 1981). In fact [see Eq. (9)], if $\sigma = 0$, $K_2[M^{++}]_0 = 1$ and, since $\Psi_0 = 0$ at that moment, one obtains $K_2 = 1/[M^{++}]_\infty$. In the present example, $K_2 = 8.5$ M^{-1} so that the surface charge will equal zero when $[M^{++}]_\infty = 0.118$ M and will become positive for higher values of $[M^{++}]_\infty$. This is true for any value of concomitant cation $[M^+]_\infty$ and for any surface concentration $\{R_{tot}\}$.

The Electrical Potential

Whether or not the surface potential (the electrical potential at the surface) is related to the membrane potential is a largely debated question. As stressed by Hashimoto and Rottenberg (1983) and Hashimoto *et al.* (1984), this is more a question of finding an adequate technique to measure the surface potential correctly. The relation has been demonstrated for plant vacuoles (Barbier-Brygoo *et al.*, 1984). The spatial aspect of the electric effects near a charged surface will be discussed in the paragraph dealing with the diffuse layer. The surface potential acting at the beginning of the diffuse layer is a function of the surface charge density and of the free solution composition. Simulations A and B of Fig. 2 illustrate these two direct effects. For any given concentration of the free solution, $|\Psi_0|$ increases with $|\sigma|$. For a given σ and in the presence of a unique electrolyte, $|\Psi_0|$ exhibits a linear decay as the logarithm of the molar concentration increases, with a 29-mV slope in the case of divalent cations and a 58-mV slope in the case of monovalent cations. A given concentration of monovalent cation induces a Ψ_0 potential which is twice the potential observed in the presence of the same molar concentration of divalent cation. If the solution consists of both electrolytes, the potential Ψ_0 is determined by the divalent cation only, provided $[M^+]_\infty < 10^{-2}$ M.

When the Stern model is considered (simulations C and D), these observations remain qualitatively true (Fig. 2). Nevertheless, the Ψ_0 values, induced by identical concentrations of monovalent and divalent cations, follow approximately a ratio of from 3/1 to 4/1, whereas this ratio was 2/1

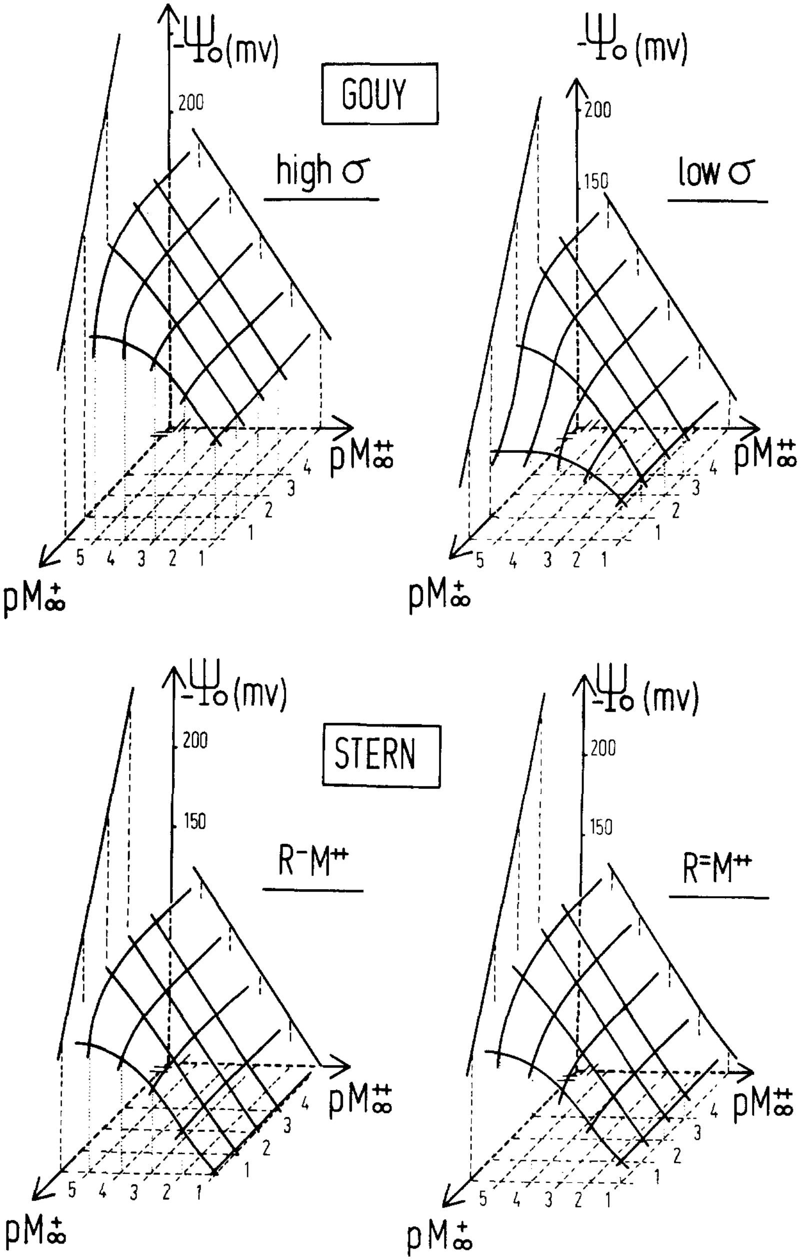

Fig. 2. Surface potential versus monovalent and divalent cation concentrations in the free solution. Two surface charges (simulation A and B, upper) and two binding mechanisms are compared (simulation C and D, lower).

in the case of the Gouy–Chapman model. In practice this means that if the potential Ψ_0 observed with a given divalent concentration, e.g., $[M^{++}]_\infty = 10^{-4}$M, is to be obtained without any divalent cation in the medium, the following monovalent cation concentrations should be applied: $[M^+]_\infty \simeq 10^{-2}$M with the Gouy–Chapman model and $[M^+]_\infty \simeq 10^{-1}$M with the Stern model. We propose to identify such concentrations as "equipotent." Thus equipotent concentrations describe concentrations of cations bearing a different valence and inducing an identical electrostatic effect. Such a concept can explain the same influence of very different $[M^+]_\infty$ and $[M^{++}]_\infty$ concentrations on a given phenomenon. Ahrens (1981, 1983) applied it successfully to the electrostatic control of the enzymatic activity of a membrane-bound enzyme.

The $|\Psi_0|$ decay for a given weak $[M^{++}]_\infty$ and an increasing $[M^+]_\infty$ is more marked in the Gouy–Chapman model than in the Stern model. This is due to the increase of $|\sigma|$ under the same circumstances (Fig. 1) which attenuates the effect of the ionic strength increase. Choosing either binding mechanisms introduces no difference for the Ψ_0 variation unless high $[M^{++}]_\infty$ values are considered. As has been mentioned, the surface charge may be reversed if R^-M^{++} complexes are formed.

Finally, due to its paradoxical appearance, the following is worth emphasizing: in the presence of low divalent cation concentrations, $[M^{++}]_\infty$ lying between 10^{-5}–10^{-4}M, if the monovalent cation concentration is increased, the surface charge σ *increases* as the potential Ψ_0 *diminishes* (Fig. 3). This experimental pathway is of peculiar interest as it permits one

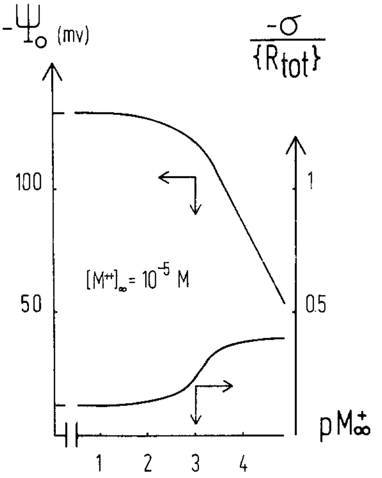

Fig. 3. Surface potential and ratio of surface charge density to total surface site concentration versus monovalent cation concentration in the free solution (simulation D).

to study the dissociation of the surface charge and the surface potential effects upon a given phenomenon.

The Concentrations at the Surface

The model permits the calculation of concentrations at any distance from the surface: $[M^z]_x$. But it is the value $[M^z]_0$ which present the greatest interest. The latter refer to volume concentrations concerning the plane $x = 0$ of the diffuse layer and are not to be confused with surface concentrations concerning the Stern layer. The former are especially important because it is these concentrations and not the concentrations in the free solution $[M^z]_\infty$ which constitute the actual electrolytic environment of any phenomenon occurring in the vicinity of a charged surface, e.g., the activity of a membrane-bound enzyme. If they are not taken into account for calculations of binding constants, these are apparent constants, so-called as opposed to intrinsic constants calculated with concentrations at the surface. Figure 4 (right) presents the concentrations at the surface $[M^{++}]_0$ and $[M^+]_0$ when a constant surface charge (Gouy–Chapman model) of 0.5×10^{-6} mol/m^2 is considered (B simulation). The simulation A (2.37×10^{-6} mol/m^2, not shown) results in concentrations at the surface of the order of 15 M which are unrealistic if the ion size is considered. In the presence of a unique electrolyte the concentrations at the surface are not dependent on the ion valence nor on the concentrations in the free solution if these do not exceed 10^{-2} M. Consequently, in the Boltzmann equation (1), variations of the concentration component are exactly compensated by reverse variations of the exponential component. In fact, as mentioned earlier, identical concentrations of monovalent and divalent cations induce, respectively, the surface potentials Ψ_0 and $\Psi_0/2$, which neutralize the valence effect.

When both electrolytes occur in the free solution, it is the sum of the concentrations at the surface $[M^{++}]_0 + [M^+]_0$ which presents this remarkable constancy. These observations illustrate particularly well the so-called "screening effect" of the diffuse layer: Simple electrostatic phenomena render the electrolytic environment of the surface insensitive to variations of the external medium (where $x = \infty$).

Within the framework of the Stern model, the preceding observations still hold when σ remains constant since it is essentially this parameter that fixes the surface concentrations. Consequently, there is no significant difference between the two binding mechanisms since the surface charge is similar in the two hypotheses (Fig. 1). Figure 4 (simulation D, left) shows that the divalent concentrations at the surface always remain weak: $[M^{++}]_0 < 0.25$ M. On the other hand, the monovalent cation concentrates mainly at the surface (up to 2.5 M) when $[M^+]_\infty$ increases and $[M^{++}]_\infty$

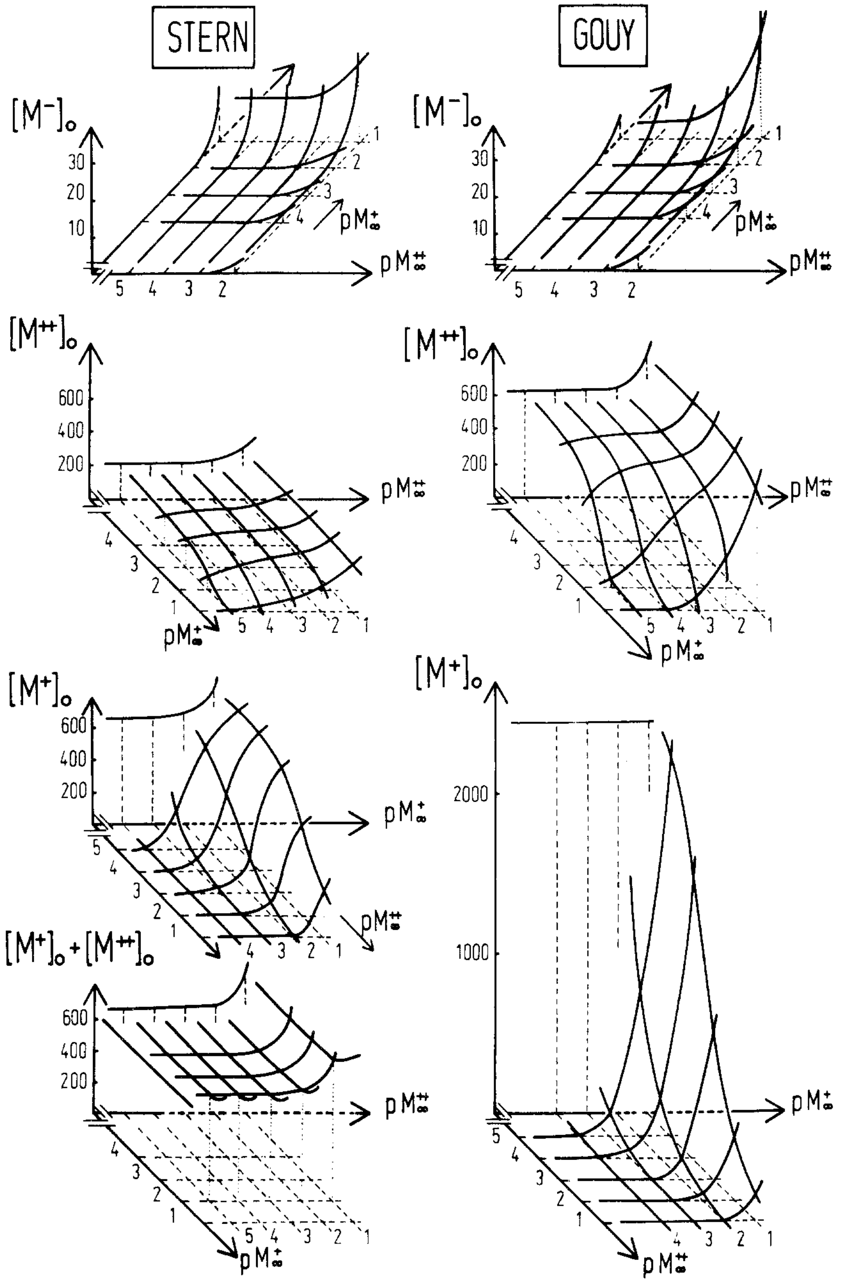

Fig. 4. Concentrations at the surface (mmol/liter) for monovalent, divalent, and sum of cations and anions versus cation concentrations in the free solution. Binding (left, simulation D) is compared with no binding (right, simulation B).

decreases. The variations of the surface concentrations constitute, as a result, a fundamental difference between a model which assumes that σ is constant (Gouy–Chapman) and a model which assumes that σ is variable (Stern).

The anion concentrations at the surface $[M^-]_0$ are of particular interest when membrane-bound enzymes react with an anionic substrate (e.g., ATPase) or when the binding of a negative fluorescent probe is studied (e.g., ANS^-). In contrast to cationic concentrations at the surface, the anionic concentrations at the surface are very sensitive to variations of the electrolytic medium (Fig. 4), since both components of the Boltzmann equation (1) vary in the same way for anions. The concentrations $[M^-]_0$ are higher than 1 mM only if $[M^+]_\infty$ reaches 10^{-1}M and $[M^{++}]_\infty$ reaches 10^{-2}M. Differences between the models are explained by σ modifications. For a given composition of the solution, $[M^-]_0$ is less if σ is greater. In short, σ excludes anions from the surface.

The Stern Layer

The surface charge density σ, which controls the electric potential and the ionic concentrations in the diffuse layer, is, in turn, controlled by the intensity and the mechanisms of specific binding of the cations with the charged sites of the surface R^- [Eqs. (7) and (8)]. Figure 5 represents the evolution of the complexation level of the R sites as either of the two binding mechanisms is considered for divalent cations. The surface concentration of the complexed monovalent cations $\{R^-M^+\}$ becomes significant only if $[M^+]_\infty > 10^{-2}$M and if $[M^{++}]_\infty < 10^{-2}$M. Such a behavior is linked to the variation of $[M^+]_0$ (Fig. 4). The concentration $\{R^-M^+\}$ is practically insensitive to the choice of a divalent binding mechanism. The divalent cation concentrations in the Stern layer $\{R^-M^{++}\}$ or $\{R^{-2}M^{++}\}$ are the same for both mechanisms. Such a quantitative agreement is due to the choice of the values of the constants K_2 and K_3. Nevertheless, it should be noted that the $R^{-2}M^{++}$ mechanism requires twice as many R sites as the R^-M^{++} mechanism for complexation. This accounts for the weaker surface concentration of free R^- sites with the $R^{-2}M^{++}$ mechanism (Fig. 5).

All simulations were carried out with either $K_2 = 0(\{R^-M^{++}\} = 0)$ or with $K_3 = 0(\{R^{-2}M^{++}\} = 0)$. If both mechanisms are considered simultaneously, the two complexes R^-M^{++} and $R^{-2}M^{++}$ should always be encountered in the same concentration ratio:

$$\frac{\{R^-M^{++}\}}{\{R^{-2}M^{++}\}} = 2K_2/K_3$$

The Diffuse Layer

The surface charge density σ is balanced by the ions of the diffuse layer.

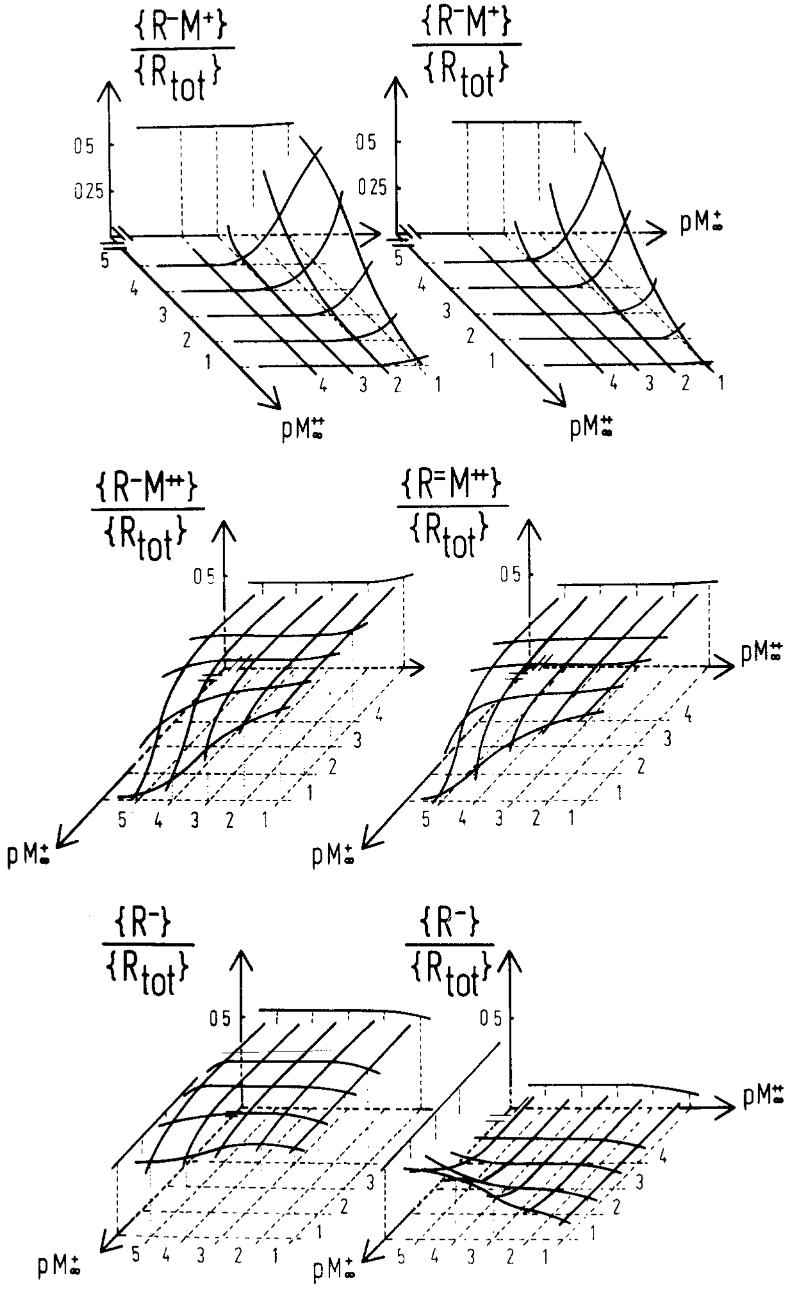

Fig. 5. Ratio of surface concentrations of possible R complexes to total surface site concentrations versus cation concentrations in the free solution. Two binding mechanisms are compared (left, simulation C; right, simulation D).

If σ is negative, neutralization is ensured by an excess of monovalent (Γ^+) and divalent (Γ^{++}) cations as well as a deficiency of monovalent anions (Γ^-). These quantities are defined by reference to the concentrations in the free solution [Eq. (13)]. Figure 6 shows how the ratios $\Gamma^+/-\sigma$, $2\Gamma^{++}/-\sigma$, and Γ^-/σ behave when a constant surface σ charge is considered. A varying surface charge case is not shown because both models can be discussed at the same time so long as the following are kept in mind: For a given composition of the solution, increasing the surface charge density decreases the proportion of monovalent cations ($\Gamma^+/-\sigma$), increases the proportion of divalent cations ($2\Gamma^{++}/-\sigma$), and decreases the negative adsorption (Γ^-/σ). In any case, the differences between the models are minimal.

The contribution of the monovalent cations to the neutralization of σ becomes significant (> 10%) only if the ratio $[M^+]_\infty/[M^{++}]_\infty$ is higher than

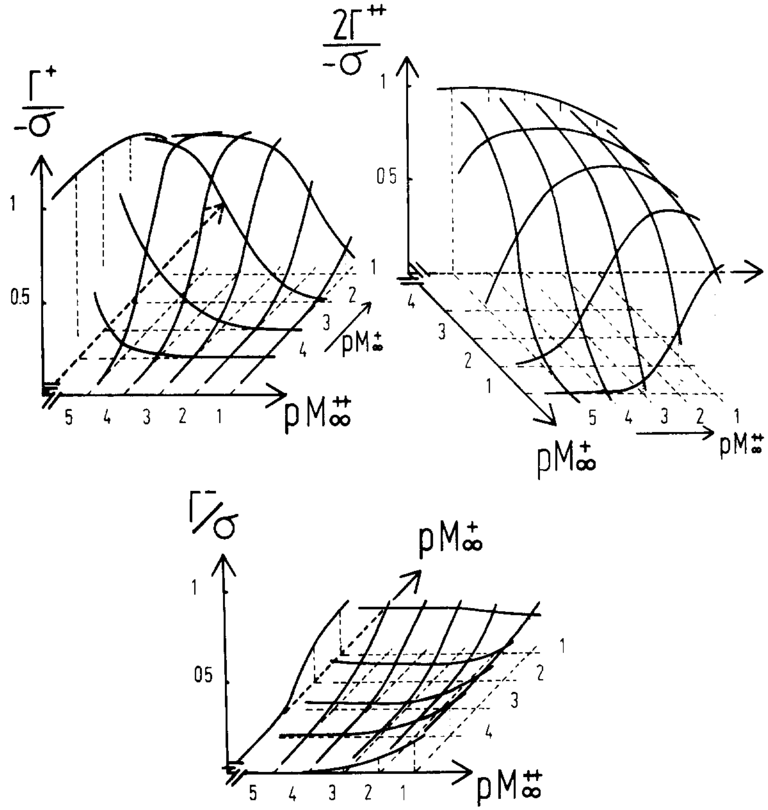

Fig. 6. Proportion of monovalent cations, divalent cations, and anions in the diffuse layer versus cation concentrations in the free solution (simulation B).

10. For an identical concentration ratio in the free solution, this contribution is more important when the ionic strength is high. On the other hand, the contribution of divalent cations is, at least, equal to 50% as soon as the ratio $[M^+]_\infty/[M^{++}]_\infty$ is smaller than 10. The dilution of the free solution favors the excess of divalent cations in the diffuse layer. These established observations remain valid, at least qualitatively, when the Stern model is considered. The specific binding mechanism R^-M^{++} or $R^{-2}M^{++}$ does not modify this assertion as the surface charge density is very similar for both mechanisms (Fig. 1). Although it is often explicitly or implicitly neglected, the contribution of the anion deficiency to the neutralization of the surface charge (i.e., the negative adsorption) is higher than 10% when $[M^+]_\infty$ and/or $[M^{++}]_\infty$ is $> 10^{-2}$ M. If the solution consists of a unique electrolyte, the limiting value of Γ^-/σ are 0.5 and 0.33 in the presence of monovalent and divalent cations, respectively.

The extent of the diffuse layer, in other words, the distance at which the surface charge causes a significant disturbance of the ionic medium, can be evaluated by the exclusion distance of the anions: $-d_{ex} = \Gamma^-/[M^-]_\infty$. It is calculated to replace the actual continuous increase of $[M^-]_x$ from $[M^-]_0$ to $[M^-]_\infty$ by a fictitious jump of $[M^-]_x$ from 0 to $[M^-]_\infty$. In other words, it is the distance at which the anion deficiency can be replaced by a complete absence of anions. In inert ion exchangers (cell walls, clays, resins, etc.), the exclusion distance permits the calculation of the extent of the "free space" (FS, ml/g) using the total hydration (H, ml/g) and the specific surface area (S, cm^2/g):

$$\mathrm{FS} = H - S \cdot d_{ex} \tag{14}$$

The simulations A ($-\sigma = 2.37 \times 10^{-6}$ mol/m^2) and B (0.5×10^{-6} mol/m^2) resulted in similar values for d_{ex}. Therefore, the thickness of the diffuse layer is independent of the surface charge density and is dependent only on the electrolytic medium. Consequently, the process of specific binding, whatever the mechanism may be, will not affect the exclusion distance d_{ex}. If the medium consists of a unique electrolyte, d_{ex} decreases sharply as the concentration is increased (Fig. 7). The valence effect is particularly obvious. Concentrations of monovalent and divalent cations in the ratio $[M^+]_\infty/[M^{++}]_\infty \simeq 10$ result in the same thickness of the diffuse layer. The "penetrating power" of the anion is much more important when it is accompanied by a divalent cation and when the ionic strength is high.

If the medium consists of both electrolytes, when $[M^{++}]_\infty \simeq 0.1$ M, d_{ex} decreases to a value close to that of a water monolayer ($\simeq 3$ Å) whatever the monovalent cation concentration may be. In such a situation, the applicability of the original diffuse layer theory becomes questionable because the ions can be considered as point charges only if the diffuse layer thickness is

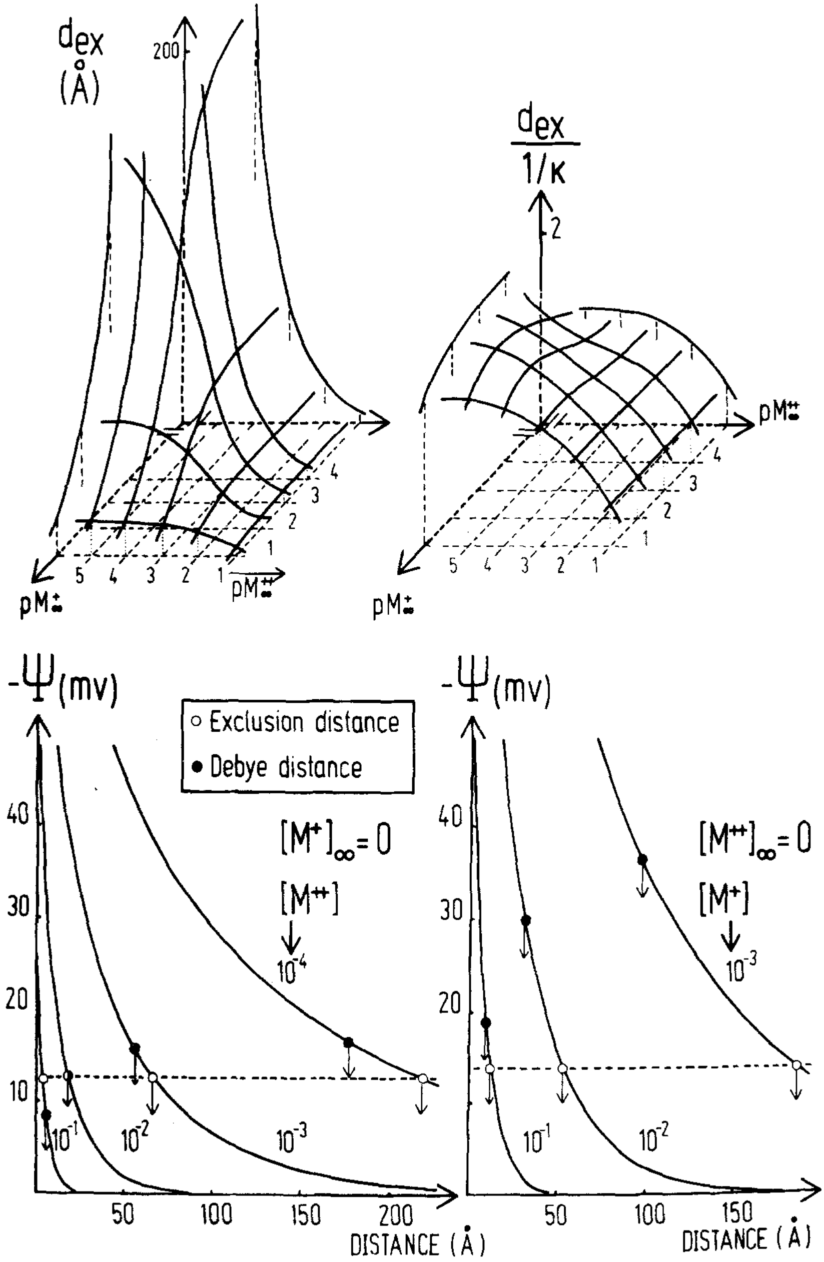

Fig. 7. Exclusion distance (upper left) and ratio of exclusion distance to Debye length (upper right) versus cation concentrations in the free solution. Surface potential versus distance from the surface (lower) with varying divalent (left) and monovalent (right) cation concentrations in the free solution (all simulations B).

much greater than the size of the hydrated ions. As mentioned earlier concerning the concentrations at the surface, the exclusion of the anions will be important in phenomena involving interactions between a negative surface (phospholipid membrane) and a negative species:

—The absorption of phosphates by plants is favored by an enhanced ionic strength of the nutrient solution (Tang Van Hai and Laudelout, 1971).

—The affinity of membrane-bound enzymes (e.g., arylsulfatase) for their negative substrate is diminished as anionic surfactants are added to the membrane, and they induce an increase of R^- sites (Nalecz *et al.*, 1983).

These simulations show a surprising and unexplained fact: The electrical potential Ψ_{ex}, where $x = d_{ex}$, results in a remarkably constant value of 13–14 mV (Fig. 7), irrespective of the σ values (with $\sigma < 0$), the concentrations of the solution, and the specific binding mechanism (Fig. 7). The Debye length $1/\kappa$ is also often used to estimate the thickness of the diffuse layer. It is defined as

$$1/\kappa = \left(\frac{\varepsilon_r \varepsilon_0 RT}{2F^2}\right)^{1/2} I^{-1/2} \tag{15}$$

where I is the ionic strength of the free solution:

$$I = 0.5 \sum z_i^2 [\mathrm{M}_i]_\infty \tag{16}$$

In systems where the surface potential is very weak ($z|\Psi_0| < 25$ mV), the potential exhibits a strictly exponential decay with distance.

$$\Psi_x = \Psi_0 \exp(-\kappa x) \tag{17}$$

and the Debye length is the distance at which the potential has fallen to $\Psi_0/2.718$. Due to its limited signficance, the Debye length gives a less accurate value of the diffuse layer thickness than the exclusion distance. On the other hand, it is very easy to calculate. This is not true for the exclusion distance which requires the calculation of the Ψ vs. x relationship. Figure 7 compares the Debye length with the exclusion distance and stresses the constant value of the potential at the latter distance in comparison with the former.

Ion-Exchange Isotherms

Generally an ion-exchange isotherm is a curve which describes the relationship of thermodynamic equilibrium between a surface phase and a free solution. The composition of these phases is often expressed in terms of equivalent ionic fractions, and an isotherm represents the equilibrium points corresponding to a constant total normality (sometimes ionic strength) of the free solution. Such a representation is seldom used in studies of biological membranes; it is often used for ion exchanges on cell walls (Van Cutsem and

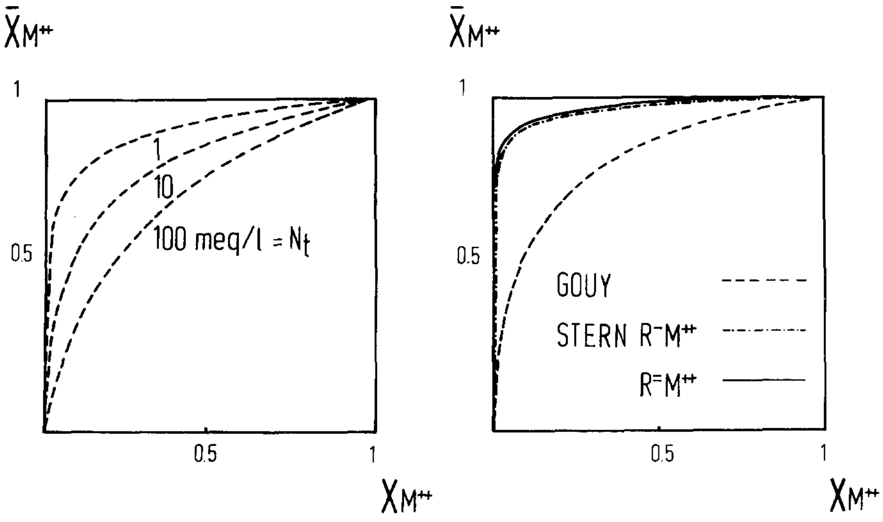

Fig. 8. Divalent–Monovalent exchange isotherms. Divalent cation equivalent surface fraction versus divalent cation equivalent fraction in solution [see Eqs. (18)–(23)]. Different total normalities, N_t, are compared (left, simulation B). Binding and no binding are compared (right, simulations B, C, and D; N_t = 10 meq/liter).

Gillet, 1981; Amory and Dufey, 1984) and is currently used in the field of ion exchange on clays and soils.

In the absence of any specific binding with the membrane (no Stern layer) Fig. 6 permits one to plot several ion-exchange isotherms corresponding to different total normalities of the free solution (Fig. 8, left). Adsorbed equivalent ionic fractions are defined for divalent cations as

$$\bar{X}^{++} = 2\Gamma^{++}/(\Gamma^{+} + 2\Gamma^{++}) \tag{18}$$

and for monovalent cations as

$$\bar{X}^{+} = \Gamma^{+}/(\Gamma^{+} + 2\Gamma^{++}) \tag{19}$$

with

$$\bar{X}^{++} + \bar{X}^{+} = 1 \tag{20}$$

Equivalent ionic fraction in solution are defined for divalent cations as

$$X^{++} = 2[M^{++}]_\infty/N_t = 1 - X^{+} \tag{21}$$

where N_t is the total normality:

$$N_t = 2[M^{++}]_\infty + [M^{+}]_\infty = [M^{-}]_\infty \tag{22}$$

It is obvious from Fig. 8 that the valence effect upon the selectivity is neutralized as the total normality is increased.

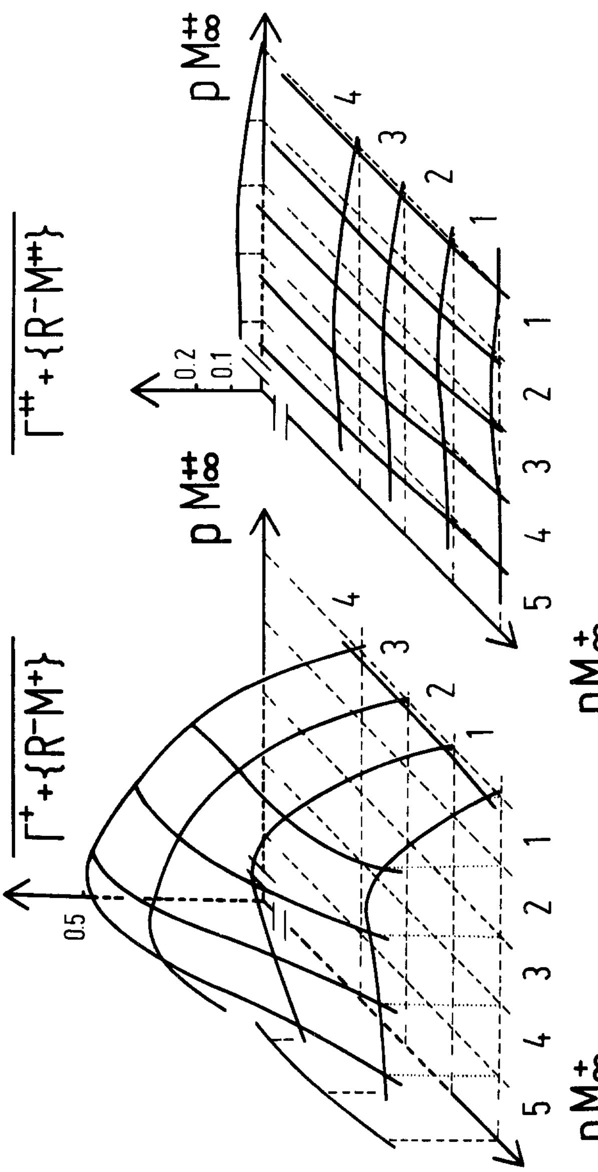

Fig. 9. Ratio of monovalent (left) or divalent cations (right) of the diffuse layer to the cation content of both layers (simulation B).

If specific bindings are considered, the adsorbed equivalent fractions consist of the cations of the diffuse layer as well as the Stern layer. Consequently,

$$
\begin{aligned}
\bar{X}^{++} &= \frac{2\{R^-M^{++}\} + 2\{R^{-2}M^{++}\} + 2\Gamma^{++}}{2\{R^-M^{++}\} + 2\{R^{-2}M^{++}\} + \{R^-M^+\} + 2\Gamma^{++} + \Gamma^+} \\
&= 1 - \bar{X}^+ \qquad (23)
\end{aligned}
$$

Figure 8 presents an ion-exchange isotherm calculated from (23). The selectivity in favor of the divalent cation is important irrespective of the complexation mechanism considered. This could be predicted as the higher capacity of the divalent cation to form complexes in the Stern layer (Fig. 5) is added to its exchange selectivity in the diffuse layer (Fig. 6). This selectivity increment in favor of the divalent cation is stressed in Fig. 9 which shows the distribution of the cations between the diffuse and the Stern layer. More than 90% of the adsorbed divalent cations occur in the Stern layer. On the other hand, a significant proportion of the adsorbed monovalent cations occur in the diffuse layer. For a given $[M^+]_\infty$ concentration in solution, this proportion reaches a maximum value as $[M^{++}]_\infty$ is increased. The maximum occurs earlier if weaker $[M^+]_\infty$ are used. For a given $[M^{++}]_\infty$ the proportion of monovalent cations in the diffuse layer decreases as $[M^+]_\infty$ increases. This seems paradoxical since $|\sigma|$ and $[M^+]_\infty$ increase together (Fig. 2) and the extent of the diffuse layer is proportional to σ. This means that the monovalent cation concentration in the Stern layer $\{R^-M^+\}$ (Fig. 6) increases more rapidly than the concentration in the diffuse layer Γ^+.

Summary

In conclusion, we stress the following points:

—The model permits the biologist who is unfamiliar with surface chemistry to examine together all the properties originating from the formation of a Stern layer and a diffuse layer.

—The three-dimensional figures presented permit researchers working with biomembranes to choose adequate experimental conditions in order to avoid or to elucidate problems arising from surface phenomena.

—The model can also be used in a quantitative way to simulate or evaluate data in terms of the Stern theory. The parameters which must be measured or estimated are the association constants and the total surface charge. Calculations[4] are performed with the help of a microcomputer.

---

[4] The program used (BASIC) and an example of the output may be obtained from the authors.

References

Abraham-Shrauner, B. (1975). *J. Math. Biol.* **2**, 333–339.

Abraham-Shrauner, B. (1977). *J. Math. Biol.* **4**, 201.

Ahrens, M. L. (1981). *Biochim. Biophys. Acta* **642**, 252–266.

Ahrens, M. L. (1983). *Biochim. Biophys. Acta* **732**, 1–10.

Alvarez, O., Brodwick, M., Latorre, R., McLaughlin, A., McLaughlin, S., and Szabo, G. (1983). *Biophys. J.* **44**, 332–342.

Amory, D. E., and Dufey, J. E. (1984). *Plant Soil*, **80**, 181–190.

Arnold, P. W. (1978). In *The Chemistry of Soil Constituents* (Greenland, D. J., and Hayes, M. H. B., eds.), Wiley, London, pp. 355–404.

Aveyard, R., and Haydon, D. A. (1973). *An introduction to the Principles of Surface Chemistry*, Cambridge University Press, London and New York.

Barbier-Brygoo, H., Romieu, C., Grouzis, J. P., Gibrat, R., Grignon, C., and Guern, J. (1984). *Z. Pflanzenphysiol.* **114**, 215–221.

Bolt, G. H. (1979). *Soil Chemistry.* B: *Physico-chemical Model* (Bolt, G. H., ed.), Elsevier Scientific Publishing Company, Amsterdam, London, and New York.

Carnie, S., and McLaughlin, S. (1983). *Biophys. J.* **44**, 325–332.

Caspers, J., Goormaghtigh, E., Ferreira, J., Brasseur, R., Vandenbranden, M., and Ruysschaert, J. M. (1983). *J. Colloid. Interface Sci.* **91**, 546–551.

Chapman, O. L. (1913). *Philos. Mag.* **25**, 475–481.

Chiu, V. C. K., Mouring, D., Watson, B. D., and Haynes, D. H. (1980). *J. Membr. Biol.* **56**, 121–132.

Cunningham, C. C., and Sinthusek, G. (1979). *Biochim. Biophys. Acta* **550**, 150–153.

Ehrenberg, B., and Berezin, Y. (1984). *Biophys. J.* **45**, 663–670.

Eisenberg, M., Gresalfi, T., Riccio, T., and McLaughlin, S. (1979). *Biochemistry* **18**, 5213–5223.

Eriksson, E. (1952). *Soil Sci.* **74**, 103–113.

Ferreira, J., Caspers, J., and Ruysschaert, J. M. (1984). In *Charge and Field effects in Biosystems* (Allen, M. J., and Usherwood, P. N. R., eds.), Abacus Press, Turnbridge, Wells, England, pp. 157–169.

Gibrat, R., and Grignon, C. (1982). *Biochim. Biophys. Acta* **692**, 462–468.

Gouy, M. (1910). *J. Phys. (Paris)* **9**, 457–468.

Grahame, D. C. (1947). *Chem. Rev.* **41**, 441–501.

Hashimoto, K., and Rottenberg, H. (1983). *Biochemistry* **22**, 5738–5745.

Hashimoto, K., Angiolillo, P., and Rottenberg, H. (1984). *Biochim. Biophys. Acta* **764**, 55–62.

Haynes, D. H. (1974). *J. Membr. Biol.* **17**, 341–365.

Hossack, J. A., Wheeler, G. E., and Rose, A. H. (1972). *Proceedings of the International Symposium on Yeast Protoplasts*, Salamanca, 1972 (Villanueva, J. R., Garcia-Acha, I., Gascon, S., and Uruburu, F. eds.), Academic Press, London and New York.

Lakhdar-Ghazal, F., Tichadou, J. L., and Tocanne, J. F. (1983). *Eur. J. Biochem.* **134**, 531–537.

Lau, A., McLaughlin, A., and McLaughlin, S. (1981). *Biochim. Biophys. Acta* **645**, 279–292.

Levine, S., and Outhwaite, C. W. (1978). *J. Chem. Soc. Faraday Trans.* **74**, 1670–1689.

McLaughlin, A., Grathwohl, C., and McLaughlin, S. (1978). *Biochim. Biophys. Acta* **513**, 338–357.

McLaughlin, A . Eng, W. K., Vaio, G., Wilson, T., and McLaughlin, S. (1983). *J. Membr. Biol.* **76**, 183–193.

McLaughlin, S. (1977). *Current Topics in Membrane Transport*, Academic Press, New York, Vol. 9, pp. 71–144.

McLaughlin, S., and Harary, H. (1974). *Biophys. J.* **14**, 200–208.

McLaughlin, S., Szabo, G., and Eisenman, G. (1971). *J. Gen. Physiol.* **58**, 667–687.

McLaughlin, S., Murline, N., Gresalfi, T., Vaio, G., and McLaughlin, A. (1981). *J. Gen. Physiol.* **77**, 445–473.

Nalecz, M. J., Zborowski, J., Famulski, K. S., and Wojtczak, L. (1983). *Eur. J. Biochem.* **112**, 75–80.

Ohki, S., and Sauve, R. (1978). *Biochim. Biophys. Acta* **511**, 377–387.

Ohki, S., and Kurland, R. (1981). *Biochim. Biophys. Acta* **645**, 170–176.

Robertson, D. E., and Rottenberg, H. (1983). *J. Biol. Chem.* **258**, 11039–11048.
Roomans, G. M., and Borst-Pauwels, G. W. F. H. (1978). *J. Theor. Biol.* **73**, 453–468.
Roomans, G. M., and Borst-Pauwels, G. W. F. H. (1979). *Biochem. J.* **178**, 521–527.
Sposito, G. (1981). *The Thermodynamics of Soil Solutions*, Clarendon Press, Oxford.
Stern, O. (1924). *Z. Elektrochem.* **30**, 508–516.
Tang Van Hai, and Laudelout, H. (1971). *J. Exp. Bot.* **23**, 830–836.
Theuvenet, A. P. R., and Borst-Pauwels, G. W. F. H. (1976). *J. Theor. Biol.* **57**, 313–329.
Theuvenet, A. P. R., Van de Wijngaard, W. M. H., Van de Rijke, K. E., and Borst-Pauwels, G. W. F. H. (1984) *Biochim. Biophys. Acta*, **775**, 161–168.
Van Cutsem, P., and Gillet, C. (1981). *Plant Soil* **62**, 367–375.
Van Cutsem, P., and Gillet, C. (1982). *J. Exp. Bot.* **33**, 847–853.
Van Olphen, H. (1977). *An Introduction to Clay Colloid Chemistry*, Wiley, New York.
Verwey, E. J. H., and Overbeek, J. T. G. (1948). *Theory of Stability of Hydrophobic Colloids*, Elsevier, Amsterdam.
Wojtczak, L., and Nalecz, J. (1979). *Eur. J. Biochem.* **94**, 99–107.